Exciton delocalization, charge transfer, and electronic coupling for singlet excitation energy transfer between stacked nucleobases in DNA: An MS-CASPT2 study

Lluís Blancafort and Alexander A. Voityuk

Citation: The Journal of Chemical Physics **140**, 095102 (2014); doi: 10.1063/1.4867118
View online: http://dx.doi.org/10.1063/1.4867118
View Table of Contents: http://scitation.aip.org/content/aip/journal/jcp/140/9?ver=pdfcov
Published by the AIP Publishing

Exciton delocalization, charge transfer, and electronic coupling for singlet excitation energy transfer between stacked nucleobases in DNA: An MS-CASPT2 study

Lluís Blancafort[1,a)] and Alexander A. Voityuk[1,2,b)]
[1]*Institut de Química Computacional i Catàlisi (IQCC) and Departament de Química, Universitat de Girona, Campus de Montilivi, 17071 Girona, Spain*
[2]*Institució Catalana de Recerca i Estudis Avançats (ICREA), Barcelona 08010, Spain*

(Received 27 December 2013; accepted 18 February 2014; published online 4 March 2014)

Exciton delocalization and singlet excitation energy transfer have been systematically studied for the complete set of 16 DNA nucleobase dimers in their ideal, single-strand stacked B-DNA conformation, at the MS-CASPT2 level of theory. The extent of exciton delocalization in the two lowest (π,π^*) states of the dimers is determined using the symmetrized one-electron transition density matrices between the ground and excited states, and the electronic coupling is calculated using the delocalization measure and the energy splitting between the states [see F. Plasser, A. J. A. Aquino, W. L. Hase, and H. Lischka, J. Phys. Chem. A **116**, 11151–11160 (2012)]. The calculated couplings lie between 0.05 eV and 0.14 eV. In the B-DNA conformation, where the interchromophoric distance is 3.38 Å, our couplings deviate significantly from those calculated with the transition charges, showing the importance of orbital overlap components for the couplings in this conformation. The calculation of the couplings is based on a two-state model for exciton delocalization. However, in three stacks with a purine in the 5′ position and a pyrimidine in the 3′ one (AT, GC, and GT), there is an energetically favored charge transfer state that mixes with the two lowest excited states. In these dimers we have applied a three-state model that considers the two locally excited diabatic states and the charge transfer state. Using the delocalization and charge transfer descriptors, we obtain all couplings between these three states. Our results are important in the context of DNA photophysics, since the calculated couplings can be used to parametrize effective Hamiltonians to model extended DNA stacks. Our calculations also suggest that the 5′-purine-pyrimidine-3′ sequence favors the formation of charge transfer excited states. © *2014 AIP Publishing LLC*. [http://dx.doi.org/10.1063/1.4867118]

I. INTRODUCTION

Excitation energy transfer (EET) and excitonic interactions are the subject of great current attention because of their importance in multichromophoric systems. In EET, the electronic excitation is transferred from a donor to an acceptor chromophore. In turn, excitonic states, in particular excitonic resonance states, arise when the excitation is a combination of locally excited states on different chromophores, giving way to delocalized excited states.[1] These phenomena are very important in natural systems. For instance, excitonic interactions are relevant in the photophysics of DNA,[2,3] which is the main subject of our study, and EET is an essential step in photosynthesis.[4] Excitonic interactions also play a key role in organic electronic devices,[5] including organic light-emitting diodes[6] or photovoltaic systems with organic sensitizers.[7] In these examples, the key quantity behind EET and exciton delocalization is the electronic coupling.[8] This magnitude determines the EET rate between donor and acceptor, and the degree of excitation delocalization between chromophores. Therefore, the couplings are essential to understand the photophysics of multichromophoric systems such as those mentioned above.

Broadly speaking, there are two approaches to calculate excitonic coupling, as it has been reviewed recently.[9] The first approach is based on the partition of the coupling in three contributions, the Coulomb, exchange, and overlap terms. Each of these terms can be calculated using physical models or quantities extracted from *ab initio* calculations. Here one of the most common approaches is the calculation of the Coulomb couplings using the transition density,[10] in particular using the atomic transition charge density (in short, the transition charges).[11] The second approach is based on a transformation of the eigenstates of the Hamiltonian to a diabatic basis. In this case one obtains directly the whole couplings and not their components. The difficulty in this case lies in defining the transformation, as we explain below in detail. This approach is at the basis of energy-splitting based schemes, where the coupling is estimated from the energy splittings between the excited states of the coupled system. Although this is the most straightforward way to obtain the couplings, it has the limitation that it can only be applied to symmetric systems. Recently, Hsu *et al.*[12] introduced an elegant method to estimate the coupling for excitation energy transfer, the fragment excitation difference (FED) scheme. This scheme uses the so-called excitation density, which can be viewed as a sum of the attachment and detachment electron densities.[49] The FED scheme, which is based on the fragment

a)Electronic mail: lluis.blancafort@udg.edu
b)Electronic mail: alexander.voityuk@icrea.cat

charge difference (FCD) method for electron transfer coupling,[13] holds exactly in the case of the configuration interaction of singly excited states (CIS) scheme, where there are no configurations including two-electron and higher excitations. For other methods including these excitations, in particular multi-reference ones, it should give a reasonable estimate if the electronic excitation can be well described by a one-electron transition. However, no approach has been yet given to obtain the exact attachment and detachment densities for multi-reference methods. To overcome this limitation, Plasser, Lischka and co-workers have introduced an alternative where the couplings are derived from the energy splitting between the excited states and the extent of exciton delocalization between the fragments.[14]

Turning our attention to the photophysics of DNA, the importance of excitonic interactions and EET in the polymer is evident from the difference with respect to the isolated bases.[3,15–17] The excited state lifetimes of the isolated bases lie in the sub-ps regime and are thought to be responsible for the photostability of the DNA components.[18] In contrast, the lifetimes of the excited states of small oligomers or DNA itself are larger by several orders of magnitude. Excitonic and charge transfer states have been made responsible for this difference, and the role of these states has been discussed extensively on the basis of experimental[2,3,15–17,19–25] and theoretical[14,24,26–28] work. Most theoretical *ab initio* approaches on the excited states of DNA have considered small polymers, for which the excited states are calculated using time-dependent density functional theory[24,26–28] (TD-DFT) or wave function based methods.[14] The excited state studies are often preceded by molecular dynamics calculations to account for the structural fluctuations of the polymer. Due to its computational cost, this approach is only feasible at present for systems made of a few tens of nucleobases. In this context, the calculation of electronic coupling is important, since it provides the basis to parametrize computationally more efficient models, based on exciton theory, that may allow the treatment of larger systems. However, there are only few studies up to date dedicated to the calculation of the couplings for the nucleobases. In several of these studies, the electronic couplings have been approximated by their Coulomb contribution (the so-called dipolar couplings). Thus, Markovitsi and co-workers[29] have obtained the dipolar couplings using the atomic transition charge-distribution model and have used the couplings to simulate the UV spectra of a $(dA)_{10}\cdot(dT)_{10}$ duplex. Similarly, Czader and Bittner have calculated the spectra of a $(A)_{12}\cdot(T)_{12}$ duplex.[30] In their case, the Coulomb contribution to the couplings has been obtained with the transition density cube method. In contrast, Ritze and co-workers have obtained the electronic couplings for homodimer and -trimer nucleobase complexes, using the energy-based scheme and the second order approximate coupled-cluster singles and doubles method with restriction of identity, i.e., (RI)-CC2.[31] More recently, Kistler and co-workers have estimated the couplings for some model dimers using the transition density charges from TD-DFT and CIS.[32] Finally, Lischka and co-workers have calculated the electronic couplings between the nucleobase dimers and tetramers of two alternating DNA duplexes, using the approach outlined above implemented at the algebraic diagrammatic construction level of theory to second order with restriction of identity, (RI)-ADC(2).[14]

While these studies consider excitonic interactions in selected dimers, to date there has been no systematic investigation of the couplings for singlet excitation energy transfer between the DNA nucleobases considering all possible dimers. Such a study is necessary to understand EET in natural systems where the bases are not regularly distributed, and it is the main aim of our paper. We use the state-of-the-art multi-state complete-active-space second-order perturbation (MS-CASPT2) level of theory to calculate the electronic couplings for the complete set of 16 DNA nucleobase intra-stacked dimers in the ideal B-DNA conformation. The couplings are calculated with a modified procedure from that introduced in Ref. 14, based on an exciton delocalization descriptor. We focus on the couplings between the lowest (π,π^*) states, which are expected to have the main role in the photophysics. The states of (n,π^*) character are only weakly coupled to the (π,π^*) states and have not been considered here. The purpose of our calculations is not an accurate characterization of the electronic spectrum of the dimers, since we have used active spaces of moderate size in the complete active space self consistent field (CASSCF) wave function to reduce the computational effort. Instead of this, our goals are to prove the validity of the exciton based approach for the calculation of the couplings and to investigate systematically the lowest excited states of the dimers, focusing on electronic coupling, exciton delocalization and the role of charge transfer states. In the ideal B-DNA conformations of our study, the two lowest (π,π^*) states can be described in most cases with a model of two coupled diabatic, localized states. The couplings lie in a range of 0.02–0.14 eV, and the adiabatic states range from well localized states to almost evenly distributed excitons. In three cases, where a purine base is in the 5′ and a pyrimidine base in the 3′ position, the two lowest states have significant charge transfer character, and the situation must be described with a three state model that includes the charge transfer state, together with the locally excited states. Our theoretical development also shows that the couplings can be obtained in a straightforward way from only two quantities, the adiabatic energy splitting and an exciton delocalization index. The couplings obtained in this way differ significantly from those obtained using the transition density charges.

II. METHODS

A. Energy-splitting scheme

We start from the two-state model, which is commonly invoked for treating two-chromophore systems. For symmetry-equivalent chromophores, the EET electronic coupling V is one half of the splitting ΔE_{mn} of adiabatic states with the energies E_m and E_n,

$$|V| = \frac{\Delta E_{mn}}{2} = \frac{|E_m - E_n|}{2}, \tag{1}$$

calculated at the crossing point. Because the crossing points for large systems are difficult to localize, the adiabatic splitting is estimated for some reasonable structures. In most

cases, however, the system of interest has no symmetry and the half-splitting scheme gives only the upper limit for the coupling.

B. Exciton delocalization based coupling

In a more general approach, one uses a unitary transformation **U**, which connects the Hamiltonian of the system in the adiabatic and diabatic representations, to derive the coupling V:

$$\begin{pmatrix} \varepsilon_A & V \\ V & \varepsilon_B \end{pmatrix} = \mathbf{U} \begin{pmatrix} E_m & 0 \\ 0 & E_n \end{pmatrix} \mathbf{U}^{+}, \tag{2}$$

where E_{m} and E_{n} are the adiabatic energies of the states m and n, involved in the EET, and ε_A and ε_B the energies of the diabatic states localized on fragments A and B. We note that the diabatic states obtained by rotation of the corresponding adiabatic states are orthonormal by definition. The difficulty in calculating the coupling lies in the fact that the transformation is not unambiguously defined, since in general there is no rigorous definition of diabatic states for polyatomic molecules.[33]

In our approach, which is a modification of that from Ref. 14, we use an exciton delocalization index to define the transformation. The working formula is

$$|V| = \frac{\Delta E_{mn}}{2} \left(x_m(A)\, x_m(B)\, x_n(A)\, x_n(B)\right)^{1/4}, \tag{3}$$

where $x_m(A)$ and $x_m(B)$ are the extent of the exciton localization on the fragments A and B in the excited state ψ_{m}. This excitation localization measure, used by Lischka and co-workers,[34] was introduced by Luzanov and co-workers[35] and has the form:

$$x_m(A) = \frac{1}{2} \sum_{i,j \in A} \left[(\mathbf{S}\mathbf{P}^{0m})_{ij} (\mathbf{P}^{0m}\mathbf{S})_{ij} \right], \tag{4}$$

where **S** is the atomic orbital overlap matrix and $\mathbf{P}^{0m}$ the symmetrized one-electron transition density matrix between states 0 and m. Similarly, $x_n(A)$ and $x_n(B)$ are estimated for the excited state ψ_{n}. In its turn, the overall charge transfer measure is given by

$$x_{CT,m} = \sum_{\substack{i \in A \\ j \in B}} \left[(\mathbf{S}\mathbf{P}^{0m})_{ij} (\mathbf{P}^{0m}\mathbf{S})_{ij} + (\mathbf{S}\mathbf{P}^{0m})_{ji} (\mathbf{P}^{0m}\mathbf{S})_{ji} \right]. \tag{5}$$

In the CIS case, the sum of the exciton localization and charge transfer measures is one. In the CASSCF case, which is at the basis of our present approach, this sum is smaller than one because two electron and higher excitations are not included in the descriptors.

To derive the coupling, the exciton localization terms $x_m(I)$ can be used to define the diabatization matrix **U** of Eq. (1). In the two-state model, this matrix has the familiar form:

$$\mathbf{U} = \begin{pmatrix} \cos\omega & -\sin\omega \\ \sin\omega & \cos\omega \end{pmatrix}. \tag{6}$$

Applying the transformation to the states, the adiabatic states can be expresses in terms of the diabatic ones as

$$\begin{aligned} \psi_1 &= \varphi_A \cos\omega + \varphi_B \sin\omega, \\ \psi_2 &= \varphi_A \sin\omega - \varphi_B \cos\omega. \end{aligned} \tag{7}$$

This suggests that the transformation matrix elements can be expressed in terms of the exciton localization indices, namely:

$$\begin{aligned} x_m(A) &= \cos^2\omega, \\ x_m(B) &= \sin^2\omega. \end{aligned} \tag{8}$$

On the other hand, from Eq. (2) it follows that the couplings are

$$|V| = \frac{\Delta E_{mn}}{2} \sin(2\omega) = \Delta E_{mn} \cos\omega \ \sin\omega, \tag{9}$$

Using Eq. (8), the coupling can be expressed as a function of the exciton localization indices:

$$|V| = \Delta E_{mn} \sqrt{x_m(A)\, x_m(B)} = \Delta E_{mn} \sqrt{x_n(A)\, x_n(B)}. \tag{10}$$

In Eq. (10), $x_p(A)$ and $x_p(B)$ are the exciton localization indices on fragments A and B, calculated for state $p = m, n$. In the two-state model, the sum of $x_p(A)$ and $x_p(B)$ is exactly one and the equality between the expressions calculated using states m and n holds exactly. However this is not the case in practice. As an effective way to account for the deviation from the two-state model, we use an average value for the coupling, taking the geometric mean of the couplings calculated for the two states. This leads to Eq. (3). Alternatively one may use the arithmetic mean. In the case where the sum of $x_p(A)$ and $x_p(B)$ differs significantly from one, we extend the treatment to a three-state model (see below).

The difference between our scheme and that used in Ref. 14 is that here the transformation matrix **U** (Eq. (8)) is based only on the delocalization indices, whereas the transformation in Ref. 14 is based on a descriptor that contains the sum of the delocalization indices on the fragments and the charge transfer contributions. The separation between delocalization and charge transfer descriptors in our scheme allows us to extend it to a three-state model below.

The coupling elements can be also expressed in relation with a delocalization index L_m. L_m is a quantitative measure of exciton distribution over two fragments A and B, in state m:

$$L_m = \frac{1}{x_m^2(A) + x_m^2(B)}. \tag{11}$$

If the exciton is entirely localized on one subsystem, $L_m = 1$. the maximum value $L_m = 2$ indicates perfect delocalization between fragments A and B.

From Eq. (8), it follows that

$$L_m = \frac{1}{\cos^4\omega + \sin^4\omega}, \tag{12}$$

which gives

$$(\sin 2\omega)^2 = 2\left(1 - \frac{1}{L_m}\right). \tag{13}$$

Substituting in Eq. (10), it follows that

$$|V| = \Delta E_{mn}\left(\frac{1}{2} - \frac{1}{2L_m}\right)^{1/2}. \quad (14)$$

This equation shows that the coupling depends on the energy splitting, modulated by the amount of exciton delocalization. Equation (14) can be further developed to account explicitly for small deviations from the two-state model, as discussed for Eq. (10).

An interesting question is the relation between the dynamic diabatic states ψ_i and ψ_j which minimize the coupling $\langle\psi_i|\nabla_R|\psi_j\rangle$ and the "chemical" diabatic states corresponding to initial and final states in electron or exciton transfer processes and (almost) completely localized on the donor and acceptor states. This issue was considered in detail by Pavanello and Neugebauer[36] and Subbotnik *et al.*[37,38] and will not be addressed in the present paper.

C. Extension to a three-state model

In the case where the exciton states have substantial charge transfer character, the two-state model (Eq. (2)) can be extended to a three-state model including the charge transfer state. In this case, the diabatization transformation is given by

$$\begin{pmatrix} \varepsilon_A & V & V_{A,CT} \\ V & \varepsilon_B & V_{B,CT} \\ V_{A,CT} & V_{B,CT} & \varepsilon_{CT} \end{pmatrix} = \mathbf{U}\begin{pmatrix} E_l & 0 & 0 \\ 0 & E_m & 0 \\ 0 & 0 & E_n \end{pmatrix}\mathbf{U}^+, \quad (15)$$

where ε_{CT} is the diabatic energy of the charge transfer state and $V_{I,CT}$ are the couplings between the diabatic locally excited states and the charge transfer state. In this case, the equivalency between the diabatic and adiabatic states, e.g., for state l, is given by

$$\psi_l = u_{A,l}\varphi_A + u_{B,l}\varphi_B + u_{CT,l}\varphi_{CT}. \quad (16)$$

The squares of the coefficients u in Eq. (16) should correspond to the localization and charge transfer components of the state ψ_l, i.e.,

$$\begin{aligned} x_l(A) &= u^2_{A,l}, \\ x_l(B) &= u^2_{B,l}, \\ x_{CT,l} &= u^2_{CT,l}. \end{aligned} \quad (17)$$

These components are known for the excited states of interest from the analysis of the transition density. Using the adiabatic energies E_p and the quantities x_p(A), x_p(B) and $x_{CT,p}$ ($p = l$, m, and n) as reference data, one can derive the diabatic parameters by minimizing the error function (sum of the deviations squared). To this end, the diabatic energies and the couplings were treated as variable parameters to minimize the deviation of the adiabatic quantities (energies E and components x, Eq. (17), that describe the character of the states) obtained by diagonalization of the diabatic Hamiltonian from the corresponding reference data stemming from the MS-CASPT2 calculation.

III. COMPUTATIONAL METHODS

The calculations are carried out at the MS-CASPT2 level of theory with the ANO-S basis set, using the 3s2p1d contraction for C, N, and O, and the 2s1p contraction for H. The number of π orbitals for the single nucleobases is 8 for cytosine and thymine, 10 for adenine, and 11 for guanine. This makes calculations with the "complete" π active space for the dimers impractical, since they would require between 16 and 22 orbitals. To lower the computational cost in a balanced way, we have reduced the number of active space orbitals on the thymine and cytosine fragments of the dimers from 8 to 4. The orbitals on the adenine and guanine fragments were reduced from 10 and 11 orbitals, respectively, to 6. As we discuss in Sec. IV, these active spaces give good approximations to the energy of the lowest excited state. This approach gives an active space of 8 electrons in 8 orbitals, i.e., (8,8), for the dimers formed by two pyrimidine bases, a (12,12) active space for those formed by two purines, and a (10,10) active space for the mixed pyrimidine-purine pairs. For the calculations, the CASSCF wave function was averaged over 4 states for the monomers and 8 states for the dimers.[50] For the MS-CASPT2 calculations, we use an imaginary shift of 0.1 a.u. and an ionization potential - electron affinity (IPEA) shift of 0.25 a.u.[51]

The exciton localization and charge transfer measures are obtained with the perturbationally modified complete active space configuration interaction (PM-CASCI) transition density matrix from the MS-CASPT2 calculation. The sum $x_m(A) + x_m(B) + x_{CT,m}$ differs from one because of the contribution of two-electron and higher excitations to the wave function. The two-electron contributions are not considered in our analysis, and the data in Table II (see below) contain the normalized indices so that $x_m(A) + x_m(B) + x_{CT,m} = 1.00$. For the calculation of the couplings using the two-state model (Eq. (3)), where $x_{CT,m}$ is negligible, the localization measures are renormalized so that $x_m(A) + x_m(B) = 1.00$.

The contribution of configurations corresponding to two-electron and higher excitations to the wave function of S_1 and S_2 can be recognized comparing the trace of the product matrix $(\mathbf{SP}^{0m})(\mathbf{P}^{0m}\mathbf{S})$ with the value of 1.00 expected for a purely one-electron transition. These values are given in Table SI in the supplementary material.[48] The average value for our set is 0.73, while the largest deviations from the ideal value are found for the excitations localized on thymine (0.52–0.70). This nucleobase appears as the one where two-electron and higher excitations contribute most to the excitation. An analysis of the two-electron transition density matrix, which is beyond the scope of this paper, is required to understand these contributions better.

We have also calculated the exciton couplings V_{tc} using $S_0 \rightarrow S_1$ transition charges q_α and q_β computed with the MS-CASPT2 method for individual nucleobases:[11]

$$V_{tc} = \sum_{\substack{\alpha\in A \\ \beta\in B}} \frac{q_\alpha q_\beta}{R_{\alpha\beta}}. \quad (18)$$

This method provides excellent results for systems where $R_{\alpha\beta} > 4$ Å but may fail for shorter distances.[4]

Experimental idealized atomic coordinates of the four bases taken from high-resolution X-ray and neutron studies were used for generating the structures.[39] The mutual positions of the nucleobases in the models studied correspond to the intra-strand arrangement in a regular (ideal) B-DNA structure, with a distance of 3.38 Å between the planes of the rings. The geometries of the systems were constructed with the program SCHNArP[40] and are given in the supplementary material.[48] In our nomenclature, XY, the first letter corresponds to the nucleobase in the 5′ position and the second one to that in the 3′ one.

IV. RESULTS AND DISCUSSION

A. Results for the monomers

The results of the MS-CASPT2 calculations for the (π,π^*) excited states of the monomers (vertical excitation energies and oscillator strengths) are shown in Table I. For adenine we show the two lowest excited states, of ^1L_a and ^1L_b character, which appear close in the spectrum. For guanine, cytosine and thymine we give the lowest excitation, which is well separated from the second (π,π^*) state. We compare our results, obtained with reduced active spaces, with previous CASPT2[41,42] and EOM-CCSD(T)[43] data. Our results are in reasonable agreement with these data. The maximum deviation is found for thymine (0.25 eV with respect to EOM-CCSD(T)), whereas in the remaining cases the agreement is better than 0.2 eV. There is also good agreement with other methods, including density functional based ones, that have been reviewed recently in the literature.[44]

B. Results for the dimers

The excitation energies, oscillator strengths, and exciton localization and charge transfer measures for the nucleobase dimers are given in Table II. We have considered a set of 16 stacked intra-strand dimers. As we discuss below, the two-state model is valid for 13 dimers. In these cases we present the data for the two lowest excited states, S_1 and S_2. For three purine-pyrimidine pairs, AT, GC, and GT, the two-state model is not valid and a three-state scheme has to be applied to derive the couplings. In this case we give the data for S_1, S_2, and S_3. We note that in all A-containing dimers the excitation on this molecule corresponds to the ^1L_b state. This is in line with the results for the monomer, where this is also the lowest (π,π^*) state. Moreover, the excitations are quite sensitive to the active space of the CASSCF function, as shown by a test calculation on the TT dimer. For this system, the data in Table II were obtained with a (8,8) active space (see Computational Details). The excitation energies obtained with a (12,12) active space differ from the (8,8) ones by approximately 0.2 eV (see Table SII in the supplementary material for details). However, the coupling obtained with the (12,12) active space is close to the (8,8) one (0.060 eV *vs* 0.053 eV, see Table III and Table SII). Thus, the couplings are less sensitive to the active space than the excitation energies and our values can be considered reliable.

For the dimers, the excitation energies of the pairs are shifted with respect to the monomers because of the exciton coupling and the neighboring effects of one nucleobase on the other (mainly electrostatic interactions). The calculated shifts lie between 0.0 and 0.3 eV, with the exception of TG. These

TABLE I. Excitation energies (E_{exc} in eV) and oscillator strengths of the nucleobase monomers calculated in this work, together with reference values.

Nucleobase	MS-CASPT2/ ANO-S (this work) E_{exc} (eV)[a]	CASPT2/ ANO-L E_{exc} (eV)[a]	EOM-CCSD(T)/ TZVP E_{exc} (eV)
A (^1L_b)	5.32 (0.086)	5.20 (0.146)[b]	5.17[c]
A (^1L_a)	5.42 (0.246)	5.30 (0.201)[b]	5.47[c]
G	5.05 (0.369)	4.93 (0.158)[d]	5.12[c]
C	4.75 (0.231)	4.68 (0.093)[b]	4.76[c]
T	5.23 (0.453)	5.06 (0.334)[b]	5.48[c]

[a]Oscillator strength in brackets.
[b]Reference 41.
[c]Reference 43.
[d]Reference 42.

TABLE II. MS-CASPT2 excitation energies (E_{exc} in eV), oscillator strengths (f), and exciton delocalization and charge transfer measures for the nucleobase dimers considered in this work.

Dimer	State S_m	E_{exc} (eV)	f	$x_m(A)$	$x_m(B)$	$x_{CT,m}$	L_m	$\|L_1 - L_2\|$
AA	S_1	5.447	0.153	0.240	0.758	0.002	1.58	0.30
	S_2	5.489	0.264	0.624	0.372	0.004	1.88	…
GG	S_1	4.855	0.422	0.004	0.980	0.016	1.01	0.01
	S_2	5.049	0.340	0.969	0.010	0.021	1.02	…
CC	S_1	4.509	0.196	0.008	0.981	0.010	1.02	0.02
	S_2	4.950	0.214	0.991	0.001	0.007	1.00	…
TT	S_1	5.237	0.095	0.585	0.396	0.019	1.93	0.04
	S_2	5.346	0.837	0.372	0.601	0.026	1.89	…
AG	S_1	4.995	0.500	0.300	0.670	0.030	1.75	0.01
	S_2	5.232	0.190	0.683	0.315	0.002	1.76	…
GA	S_1	5.160	0.411	0.968	0.015	0.017	1.03	0.02
	S_2	5.353	0.324	0.005	0.981	0.014	1.01	…
AC	S_1	4.706	0.239	0.026	0.966	0.008	1.05	0.01
	S_2	5.617	0.266	0.901	0.021	0.078	1.05	…
CA	S_1	4.935	0.265	0.990	0.007	0.003	1.01	0.04
	S_2	5.544	0.358	0.024	0.943	0.034	1.05	…
TA	S_1	5.149	0.300	0.941	0.048	0.012	1.10	0.02
	S_2	5.444	0.658	0.038	0.961	0.001	1.08	…
CG	S_1	4.409	0.179	0.993	0.002	0.004	1.00	0.00
	S_2	5.087	0.263	0.001	0.985	0.014	1.00	…
TG	S_1	5.168	0.487	0.001	0.999	0.000	1.00	0.04
	S_2	6.621	0.212	0.970	0.021	0.008	1.04	…
CT	S_1	4.790	0.267	0.915	0.073	0.013	1.16	0.03
	S_2	5.100	0.384	0.062	0.935	0.003	1.13	…
TC	S_1	4.588	0.108	0.037	0.961	0.002	1.08	0.03
	S_2	5.296	0.508	0.965	0.026	0.009	1.05	…
AT	S_1	4.954	0.304	0.040	0.643	0.317	1.12	0.88
	S_2	5.304	0.160	0.234	0.219	0.547	2.00	…
	S_3	5.581	0.272	0.729	0.009	0.262	1.02	…
GC	S_1	4.687	0.173	0.021	0.957	0.022	1.04	0.02
	S_2	5.059	0.149	0.473	0.005	0.521	1.02	…
	S_3	5.334	0.203	0.425	0.027	0.548	1.13	…
GT	S_1	4.890	0.293	0.918	0.007	0.075	1.02	0.85
	S_2	5.419	0.006	0.053	0.090	0.857	1.87	…
	S_3	5.695	0.497	0.043	0.832	0.125	1.10	…

TABLE III. Electronic couplings V_{12} in eV calculated with different methods, using the two-state model.

	|V| (eV)			
Dimer	Exciton delocalization (Eq. (3))	Energy splitting (Eq. (1))	Transition charges (Eq. (18))	TD-DFT[31]
AA	1.90×10^{-02}	2.08×10^{-02}	3.12×10^{-02}	3.4×10^{-02}
GG	1.55×10^{-02}	9.69×10^{-02}	9.03×10^{-02}	...
CC	2.58×10^{-02}	2.21×10^{-01}	6.65×10^{-02}	2.1×10^{-02}
TT	5.32×10^{-02}	5.45×10^{-02}	5.18×10^{-02}	4×10^{-03}
AG	1.10×10^{-01}	1.19×10^{-01}	8.34×10^{-03}	...
GA	1.84×10^{-02}	9.67×10^{-02}	6.79×10^{-02}	...
AC	1.40×10^{-01}	4.55×10^{-01}	2.08×10^{-01}	...
CA	6.95×10^{-02}	3.04×10^{-01}	2.37×10^{-01}	...
TA	5.96×10^{-02}	1.47×10^{-01}	6.05×10^{-02}	...
CG	2.50×10^{-02}	3.39×10^{-01}	1.34×10^{-02}	...
TG	9.63×10^{-02}	7.26×10^{-01}	1.36×10^{-02}	...
CT	7.79×10^{-02}	1.55×10^{-01}	7.68×10^{-04}	...
TC	1.23×10^{-01}	3.54×10^{-01}	5.49×10^{-02}	...

shifts are in line with the so-called non-symmetry parameters derived in previous work from TD-DFT calculations for the nucleobase homodimers in their B-DNA conformation, which range from 0.01 to −0.11 eV.[31] The diabatic excitation energies ε_I can be obtained with Eq. (2) and are provided in the supplementary material (Table SIII).[48] The differences between the diabatic excitations and those of the monomers are due to the neighboring effects and lie between 0.0 and 0.34 eV, except for TG. In the TG dimer, we find that S_2, which is localized on the T molecule, appears at 6.62 eV, more than 1 eV higher than the lowest (π,π^*) state of the monomer. For this state of the dimer, the trace of the $(\mathbf{SP}^{0m})(\mathbf{P}^{0m}\mathbf{S})$ matrix is 0.521 (see table SI). The large deviation from 1 indicates that the contributions of two-electron and higher excitations to the wave function are particularly important for this state. In turn, this seems to indicate that a larger, more flexible active space would be necessary to get a more accurate estimation of the energy of S_2 for this dimer. While this is out of the scope of our paper, the trace of the $(\mathbf{SP}^{0m})(\mathbf{P}^{0m}\mathbf{S})$ matrix appears as a diagnostic tool to detect such difficult cases, and the calculated coupling for the TC dimer should be considered with care.

The degree of exciton delocalization and the partial charge transfer character of the states can be seen from the localization and charge transfer measures $x_m(i)$ and $x_{CT,m}$, respectively. In Table II we also include the localization index L_m (see Eq. (11)). These data allow us to assess the validity of the two-state model. The two-state exciton model is valid when the charge transfer contribution is small, and when the two coupled states have approximately the same degree of delocalization L_m, with a reciprocal distribution of the excitation among the fragments. Let us first examine the charge transfer character of the states. In all cases the charge transfer character of S_1 and S_2 is smaller than 8% except for AT, GC, and GT. These cases will be treated with a three-state model below. Let us now consider the excitation distribution. To assess if the coupled states have the same distribution, we have included the difference between the localization indices L_1 and L_2 to Table II. This difference is zero in the exact two-state case. The calculated values are smaller than 0.03 in 12 examples of our set (GG, CC, TT, AG, GA, AC, CA, TA, CG, TG, CT, and TC). These cases can be safely treated with the two state model. The AA case is a limiting case, since the delocalization indices for S_1 and S_2 differ by 0.3. Since the two states have almost no charge transfer character, we attribute this difference to the proximity of the ^1L_a states. Thus, S_3 for the dimer appears at 5.755 eV, only 0.26 eV higher than S_2. The ^1L_a state mixes in different ways with S_1 and S_2, of predominant ^1L_b character. The inclusion of the ^1L_a states in the calculation of the couplings is not straightforward and is out of the scope of this paper. Therefore, the AA case is also treated with the two-state model.

The electronic couplings calculated with the delocalization index are presented in Table III. The results are compared with the couplings estimated using the energy splitting approach, and those obtained from the transition density charges for the $S_0 \rightarrow S_1$ transition of the monomers. The latter couplings include only the Coulomb contribution, whereas the ones calculated with the delocalization index also include orbital interactions. The differences between the exciton delocalization based couplings and those obtained with the other methods are significant. Thus, the energy splitting method overestimates the couplings by up to a factor of 13. In turn, the couplings obtained from the transition charges represent between 1% and 583% from those obtained from the exciton delocalization measure for the same dimer. In Table II we also include the couplings estimated by Ritze and coworkers for the AA, CC, and TT homodimers.[31] These couplings come from TD-DFT calculations, based on the energy split approach including non-symmetry parameters. The differences are also very significant here, although the conformations used in the two studies may be different.

C. Results for the AT, GC, and GT dimers

In the dimers AT, GC, and GT, the charge transfer is energetically favored. This leads to mixing of the charge transfer state with the S_1 excitations of the monomers. As a result, the three lowest excited states of the dimer have mixed exciton and charge transfer character, and the three-state model (Eq. (15)) has to be applied to obtain the couplings. The results are given in Table IV, including the couplings between the locally excited diabatic states and those between these two and the charge transfer state. They lie in the same range as the couplings for the remaining dimers.

TABLE IV. Abs. values of electronic couplings V_{12}, $V_{1,CT}$, and $V_{2,CT}$, and diabatic energies ε_1, ε_2, and ε_{CT} (in eV), obtained with the three-state model for the AT and GC dimers.[a]

Dimer	$\lvert V_{12}\rvert$	$\lvert V_{1,CT}\rvert$	$\lvert V_{2,CT}\rvert$	ε_1	ε_2	ε_{CT}
AT	9.63×10^{-02}	1.37×10^{-01}	9.99×10^{-02}	5.506	5.018	5.315
GC	8.83×10^{-02}	1.30×10^{-01}	7.18×10^{-02}	5.155	4.711	5.214
GT	9.01×10^{-02}	1.59×10^{-01}	6.55×10^{-02}	4.935	5.662	5.406

[a]Indexes 1 and 2 refer to the first and second nucleobase in the dimer.

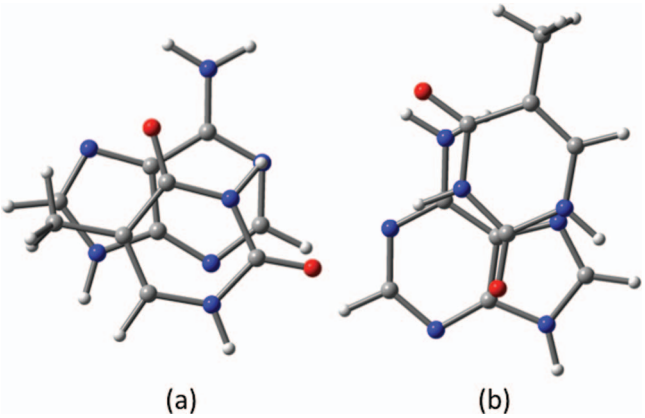

FIG. 1. (a) AT and (b) TA conformations used in our study.

The charge transfer is favored for our AT, GC, and GT conformations but not for the TA, CG, and TG ones. In TA, CG, and TG, the charge transfer states appear at 6.25 eV, 6.03 eV, and 8.23 eV, respectively. Comparison of the conformations for the AT and TA pairs (Figure 1) shows that the overlap between the rings is much better in the AT case. This appears to favor the charge transfer energetically and results in the mixed character of the three lowest states. A similar effect also occurs in the GC and GT dimers. Our results for AT and GC differ from previous calculations at different levels of theory for the same dimers in the B-DNA conformation, with a somewhat shorter stacking distance (3.38 Å here *versus* 3.15 Å in the preceding references).[45,46] In those cases, no mixing between the charge transfer and the excitonic states is reported. For example, at the EOM-CCSD(T) level of theory, the charge transfer state lies approximately 0.4 eV and 0.6 eV above the exciton states for GC and AT, respectively.[46] The difference is probably due to the different conformations used in those studies, where the mutual orientation of the rings differs from the one used here.

According to Gershgorin's theorem,[47] every eigenvalue of a matrix **H** satisfies: $|E_i - H_{ii}| \leq \sum_{j \neq i} |H_{ij}|$. In the case of a 3-state system, it implies that the adiabatic energy E_i does not deviate from the corresponding diabatic energy more than the sum of two couplings; in particular, the energy difference between an adiabatic state with an exciton largely localized on fragment 1 and the diabatic state strictly localized on this subunit is smaller than $|V_{12}| + |V_{1,CT}|$. Similar to the remaining dimers, the differences between the diabatic excitation energies and those of the monomers are smaller than 0.2 eV in all cases except for the thymine excitation energy in the GT dimer, which is 0.43 eV higher than in the monomer.

V. CONCLUSIONS

We have investigated in a systematic way singlet exciton delocalization for the complete set of 16 DNA nucleobase dimers in their ideal, single-strand stacked B-DNA conformation, and we have calculated the electronic coupling for singlet excitation energy transfer. The calculated electronic couplings lie between 0.05 and 0.14 eV. In the ideal B-DNA conformation, the stacking distance is 3.38 Å. At such a close distance, the electronic coupling has substantial contribution from the orbital overlap components, and the couplings calculated with the transition charges deviate significantly from those obtained with the exciton delocalization analysis. A similar conclusion was obtained in Ref. 32, where it was found that the Coulomb couplings give reliable values at interchromophoric distances $R > 4.5$ Å.

We have also investigated the role of low-lying charge transfer states. Such charge transfer states have been invoked in previous experimental and computational studies on DNA spectroscopy.[17,22,24,26,27,45] In the stacks AT, GC, and GT, there is a low-lying charge transfer state that mixes with the two locally excited diabatic states. In the AC dimer, the charge transfer character is not so prominent (8% for S_2). However, it is higher than for the remaining 12 dimers, where the charge transfer states appear from 9.2 eV upwards. Overall, these results suggest that the 5′-purine-pyrimidine-3′ sequence favors the formation of charge transfer states.

To calculate the couplings, we have modified the scheme for the analysis of excited states developed by Lischka and co-workers[14] and implemented it at the MS-CASPT2 level. This method assumes a two-state model, where the two adiabatic states can be reliably described by the combinations of the excitations localized on either nucleobase. The couplings are obtained as a function of the energy splitting between the adiabatic states and the extent of exciton delocalization. The method is well applicable when the excited state wave functions are dominated by one-electron excitations. In the cases where S_1 and S_2 have significant charge transfer character, a three-state scheme is applied, and the couplings between both locally excited states and the charge transfer state are obtained on the basis of the exciton localization and charge transfer indices of the three lowest states. The participation of the charge transfer states will probably be even more important when the DNA environment is included in the calculation, where these states are likely to be stabilized preferentially. To our knowledge, this is the first time where such a three-state model, providing two locally excited diabatic states and a charge transfer state, is considered. Our calculations show that these couplings cannot be neglected for the singly excited nucleobases, since the charge transfer states are low enough in energy to mix with the lowest exciton states. In the future, the method can be readily applied to investigate the conformational effect on singlet EET couplings between the DNA nucleobases and parametrize model Hamiltonians for large DNA systems which can be not treated *ab initio*. The method can also be used to study other multichromophoric systems of interest.

ACKNOWLEDGMENTS

This work was funded by the Spanish Ministerio de Economía y Competividad (MINECO) (CTQ2011-26573 and UNGI10-4E-801 from FEDER (European Fund for Regional Development)), and the Catalan Agència de Gestió d'Ajuts Universitaris i de Recerca (SGR0528) and Direcció General de la Recerca (Xarxa de Referència en Química Teòrica i Computacional de Catalunya).

[1]M. Klessinger and J. Michl, *Excited States and Photochemistry of Organic Molecules* (VCH, New York, 1995).
[2]D. Markovitsi, T. Gustavsson, and F. Talbot, Photochem. Photobiol. Sci. **6**, 717–724 (2007).
[3]C. T. Middleton, K. de La Harpe, C. Su, Y. K. Law, C. E. Crespo-Hernandez, and B. Kohler, Annu. Rev. Phys. Chem. **60**, 217–239 (2009).
[4]G. D. Scholes, Annu. Rev. Phys. Chem. **54**, 57–87 (2003).
[5]J. L. Bredas, D. Beljonne, V. Coropceanu, and J. Cornil, Chem. Rev. **104**, 4971–5003 (2004).
[6]K. Müllen and U. Scherf, *Organic Light Emitting Devices: Synthesis, Properties and Applications* (Wiley-VCH, Weinheim, 2006).
[7]D. Caruso and A. Troisi, Proc. Natl. Acad. Sci. U.S.A. **109**, 13498–13502 (2012).
[8]C.-P. Hsu, Acc. Chem. Res. **42**, 509–518 (2009).
[9]Z.-Q. You and C.-P. Hsu, Int. J. Quantum Chem. **114**, 102–115 (2013).
[10]J. C. Chang, J. Chem. Phys. **67**, 3901–3909 (1977).
[11]S. Marguet, D. Markovitsi, P. Millie, H. Sigal, and S. Kumar, J. Phys. Chem. B **102**, 4697–4710 (1998).
[12]C.-P. Hsu, Z.-Q. You, and H.-C. H. Chen, J. Phys. Chem. C **112**, 1204–1212 (2008).
[13]A. A. Voityuk and N. Rosch, J. Chem. Phys. **117**, 5607–5616 (2002).
[14]F. Plasser, A. J. A. Aquino, W. L. Hase, and H. Lischka, J. Phys. Chem. A **116**, 11151–11160 (2012).
[15]N. K. Schwalb and F. Temps, Science **322**, 243–245 (2008).
[16]I. Vaya, T. Gustavsson, F.-A. Miannay, T. Douki, and D. Markovitsi, J. Am. Chem. Soc. **132**, 11834–11835 (2010).
[17]I. Vaya, T. Gustavsson, T. Douki, Y. Berlin, and D. Markovitsi, J. Am. Chem. Soc. **134**, 11366–11368 (2012).
[18]C. E. Crespo-Hernández, B. Cohen, P. M. Hare, and B. Kohler, Chem. Rev. **104**, 1977–1202 (2004).
[19]D. Markovitsi, D. Onidas, T. Gustavsson, F. Talbot, and E. Lazzarotto, J. Am. Chem. Soc. **127**, 17130–17131 (2005).
[20]E. R. Bittner, J. Chem. Phys. **125**, 094909 (2006).
[21]F.-A. Miannay, A. Banyasz, T. Gustavsson, and D. Markovitsi, J. Am. Chem. Soc. **129**, 14574 (2007).
[22]T. Takaya, C. Su, K. de La Harpe, C. E. Crespo-Hernandez, and B. Kohler, Proc. Natl. Acad. Sci. U.S.A. **105**, 10285–10290 (2008).
[23]D. Markovitsi, T. Gustavsson, and I. Vaya, J. Phys. Chem. Lett. **1**, 3271–3276 (2010).
[24]A. Banyasz, T. Gustavsson, D. Onidas, P. Changenet-Barret, D. Markovitsi, and R. Improta, Chem. Eur. J. **19**, 3762–3774 (2013).
[25]W.-M. Kwok, C. Ma, and D. L. Phillips, J. Phys. Chem. B **113**, 11527–11534 (2009).
[26]A. W. Lange and J. M. Herbert, J. Am. Chem. Soc. **131**, 3913–3922 (2009).
[27]F. Santoro, V. Barone, and R. Improta, J. Am. Chem. Soc. **131**, 15232–15245 (2009).
[28]S. Tonzani and G. C. Schatz, J. Am. Chem. Soc. **130**, 7607–7612 (2008).
[29]E. Emanuele, D. Markovitsi, P. Millie, and K. Zakrzewska, ChemPhysChem **6**, 1387–1392 (2005).
[30]A. Czader and E. R. Bittner, J. Chem. Phys. **128**, 035101 (2008).
[31]D. Nachtigallova, P. Hobza, and H.-H. Ritze, Phys. Chem. Chem. Phys. **10**, 5689–5697 (2008).
[32]K. A. Kistler, F. C. Spano, and S. Matsika, J. Phys. Chem. B **117**, 2032–2044 (2013).
[33]C. A. Mead and D. G. Truhlar, J. Chem. Phys. **77**, 6090–6098 (1982).
[34]F. Plasser and H. Lischka, J. Chem. Theory Comput. **8**, 2777–2789 (2012).
[35]A. V. Luzanov and O. A. Zhikol, Int. J. Quantum Chem. **110**, 902–924 (2010).
[36]M. Pavanello and J. Neugebauer, J. Chem. Phys. **135**, 134113 (2011).
[37]J. E. Subotnik, R. J. Cave, R. P. Steele, and N. Shenvi, J. Chem. Phys. **130**, 234102 (2009).
[38]S. Fatehi, E. Alguire, Y. Shao, and J. E. Subotnik, J. Chem. Phys. **135**, 234105 (2011).
[39]L. Clowney, S. C. Jain, A. R. Srinivasan, J. Westbrook, W. K. Olson, and H. M. Berman, J. Am. Chem. Soc. **118**, 509–518 (1996).
[40]X. J. Lu, M. A. El Hassan, and C. A. Hunter, J. Mol. Biol. **273**, 681–691 (1997).
[41]M. Schreiber, M. R. J. Silva, S. P. A. Sauer, and W. Thiel, J. Chem. Phys. **128**, 134110 (2008).
[42]L. Serrano-Andres, M. Merchan, and A. C. Borin, J. Am. Chem. Soc. **130**, 2473–2484 (2008).
[43]P. G. Szalay, T. Watson, A. Perera, V. F. Lotrich, and R. J. Bartlett, J. Phys. Chem. A **116**, 6702–6710 (2012).
[44]M. R. Silva-Junior, M. Schreiber, S. P. A. Sauer, and W. Thiel, J. Chem. Phys. **129**, 104103 (2008).
[45]A. J. A. Aquino, D. Nachtigallova, P. Hobza, D. G. Truhlar, C. Haettig, and H. Lischka, J. Comput. Chem. **32**, 1217–1227 (2011).
[46]P. G. Szalay, T. Watson, A. Perera, V. Lotrich, and R. J. Bartlett, J. Phys. Chem. A **117**, 3149–3157 (2013).
[47]D. H. Griffel, *Linear Algebra and its Applications* (Ellis Horwood, Chichester, 1989), Vol. 1.
[48]See supplementary material at http://dx.doi.org/10.1063/1.4867118 for additional computational data for the dimers and Cartesian coordinates of the structures.
[49]M. Head-Gordon, A. M. Graña, D. Maurice, and C. A. White, J. Phys. Chem. **99**, 14261–14270 (1995).
[50]N. Forsberg and P. A. Malmqvist, Chem. Phys. Lett. **274**, 196–204 (1997).
[51]G. Ghigo, B. O. Roos, and P. A. Malmqvist, Chem. Phys. Lett. **396**, 142–149 (2004).